

10-2-2000

Optical Bandgap Formation in AlInGaN Alloys

G. Tamulaitis

K. Kazlauskas

S. Juršėnas

A. Žukauskas

M. A. Khan

See next page for additional authors

Follow this and additional works at: https://scholarcommons.sc.edu/elct_facpub



Part of the [Electromagnetics and Photonics Commons](#), and the [Other Electrical and Computer Engineering Commons](#)

Publication Info

Published in *Applied Physics Letters*, Volume 77, Issue 14, 2000, pages 2136-2138.

This Article is brought to you by the Electrical Engineering, Department of at Scholar Commons. It has been accepted for inclusion in Faculty Publications by an authorized administrator of Scholar Commons. For more information, please contact digres@mailbox.sc.edu.

Author(s)

G. Tamulaitis, K. Kazlauskas, S. Juršėnas, A. Žukauskas, M. A. Khan, J. W. Yang, J. Zhang, Grigory Simin, M. S. Shur, and R. Gaska

Optical bandgap formation in AlInGaN alloys

G. Tamulaitis, K. Kazlauskas, S. Juršėnas, A. Žukauskas, M. A. Khan, J. W. Yang, J. Zhang, G. Simin, M. S. Shur, and R. Gaska

Citation: *Applied Physics Letters* **77**, 2136 (2000); doi: 10.1063/1.1314288

View online: <http://dx.doi.org/10.1063/1.1314288>

View Table of Contents: <http://scitation.aip.org/content/aip/journal/apl/77/14?ver=pdfcov>

Published by the [AIP Publishing](#)

Articles you may be interested in

[Dielectric function and optical properties of quaternary AlInGaN alloys](#)

J. Appl. Phys. **110**, 013102 (2011); 10.1063/1.3603015

[Exciton and carrier motion in quaternary AlInGaN](#)

Appl. Phys. Lett. **82**, 4501 (2003); 10.1063/1.1586782

[Solar-blind ultraviolet photodetectors based on superlattices of AlN/AlGa\(In\)N](#)

Appl. Phys. Lett. **82**, 1323 (2003); 10.1063/1.1557325

[Growth and optical properties of \$\text{In}_x\text{Al}_y\text{Ga}_{1-x-y}\text{N}\$ quaternary alloys](#)

Appl. Phys. Lett. **78**, 61 (2001); 10.1063/1.1331087

[High optical quality AlInGaN by metalorganic chemical vapor deposition](#)

Appl. Phys. Lett. **75**, 3315 (1999); 10.1063/1.125336

High-Voltage Amplifiers

- Voltage Range from $\pm 50\text{V}$ to $\pm 60\text{kV}$
- Current to 25A

Electrostatic Voltmeters

- Contacting & Non-contacting
- Sensitive to 1mV
- Measure to 20kV



ENABLING RESEARCH AND
INNOVATION IN DIELECTRICS,
ELECTROSTATICS,
MATERIALS, PLASMAS AND PIEZOS



www.trekinc.com

TREK, INC. 190 Walnut Street, Lockport, NY 14094 USA • Toll Free in USA 1-800-FOR-TREK • (t):716-438-7555 • (f):716-201-1804 • sales@trekinc.com

Optical bandgap formation in AlInGaN alloys

G. Tamulaitis, K. Kazlauskas, S. Juršėnas, and A. Žukauskas^{a)}
Institute of MSAR, Vilnius University, Naugarduko 24, 2006 Vilnius, Lithuania

M. A. Khan, J. W. Yang, J. Zhang, and G. Simin
Department of ECE, University of South Carolina, Columbia, South Carolina 29208

M. S. Shur
Department of ECSE and CIEEM, Rensselaer Polytechnic Institute, Troy, New York 12180

R. Gaska
Sensor Electronic Technology, Inc., 21 Cavalier Way, Latham, New York 12110

(Received 20 April 2000; accepted for publication 9 August 2000)

We report on the spectral dynamics of the reflectivity, site-selectively excited photoluminescence, photoluminescence excitation, and time-resolved luminescence in quaternary AlInGaN epitaxial layers grown on GaN templates. The incorporation of a few percents of In into AlGaIn causes significant smoothening of the band-bottom potential profile in AlInGaN layers owing to improved crystal quality. An abrupt optical bandgap indicates that a nearly lattice-matched AlInGaN/GaN heterostructure with large energy band offsets can be grown for high-efficiency light-emitting devices. © 2000 American Institute of Physics. [S0003-6951(00)01440-6]

Recently, we demonstrated an energy band and lattice mismatch engineering approach using the quaternary AlInGaIn material system.^{1,2} The incorporation of In into AlGaIn layers enabled us to significantly reduce the lattice constant of the alloy and, thus, to grow nearly lattice-matched AlInGaIn/GaN heterostructures with large energy band offsets.¹ The introduction of AlInGaIn barrier layers reduced the built-in strain and piezoelectric doping in AlInGaIn/GaN heterostructures with a two-dimensional electron gas,² and significantly enhanced the light emission from AlInGaIn/InGaIn quantum-well structures and light-emitting diodes.³

The lattice match between AlInGaIn and GaN layers is achieved at Al to In ratio close to 5 to 1, in good agreement with Vegard's law. However, the energy band offset in AlInGaIn/GaN heterostructures extracted from the photoluminescence spectra is almost two times smaller than expected from the linear approximation of the energy gap in the quaternary AlInGaIn alloys and the details of the energy band formation in the quaternary alloy are not clear. The incorporation of In into AlGaIn requires reduced growth temperature in comparison with the growth of high crystalline quality AlGaIn.⁴ The growth at lower temperatures may lead to the disordering of the AlGaIn sublattice and, thus, to the degradation of the material quality. On the other hand, indium is known to improve the crystal structure of III-N layers via isoelectronic doping.^{5,6} However, to date, the ordering effects and optical properties of the quaternary AlInGaIn lack the systematic studies.

In this article, we report on a detail study of the optical bandgap in AlInGaIn layers grown on GaN templates. We measured reflectivity, site-selectively excited photoluminescence (SSEPL), photoluminescence excitation (PLE), and time-resolved luminescence (TRL). Our results demonstrate

that the incorporation of In into AlGaIn layers results in a significant improvement of the material quality and optical properties of the quaternary AlInGaIn alloy.

For this study, 200 nm thick Al_{0.09}In_yGa_{0.91-y}N epitaxial layers were grown over a basal plane sapphire substrate using a low pressure metalorganic chemical vapor deposition. The growth temperature was 850 °C. A 100 nm GaN template was deposited prior to the deposition of AlInGaIn. The Ga- and Al-precursor (TMGa and TMAI) flows were kept constant at an approximate ratio of 10. The incorporation of In was controlled by changing the flow of the In precursor, TMIn. The maximum flux of TMIn, F_{In} , was 10 $\mu\text{mol/min}$, which corresponded to the incorporation of approximately 2% of In. The detailed description of the growth conditions and sample characterization can be found in Ref. 1. The extracted values of In molar fraction did not account for possible corrections due to the biaxial and hydrostatic strain,⁷ which may depend on the degree of relaxation⁸ and on the defect density.

The reflectivity spectra were measured using a tungsten lamp. They exhibit an exciton-like structure. We used the spectra for the extraction of the exciton resonance energy by a conventional fitting procedure.⁹ The extracted resonance energies are 3.677, 3.645, and 3.566 eV for an In-precursor flux of 0, 5, and 10 $\mu\text{mol/min}$, respectively. We also estimated the exciton energy in the GaN buffer to be 3.418 eV.

The SSEPL and PLE spectra were measured using a tunable organic-dye laser pumped by the fourth harmonic of a Q-switched YAG:Nd³⁺ laser (10 ns pulse duration). A set of dyes (buthyl-PBD, BMQ, p-terphenyl, and BM-terphenyl) allowed us to cover a wide spectral range from 3.30 to 3.80 eV. The constant density of the incident photon flux of $5 \times 10^{22} \text{ cm}^{-2} \text{ s}^{-1}$ was controlled using a calibrated photodiode gauge (Ophir/PD10). The SSEPL and PLE spectra were recorded using a 0.6 m double pass monochromator and a UV-enhanced photomultiplier (Hamamatsu R1463P). The

^{a)}Electronic mail: arturas.zukauskas@ff.vu.lt

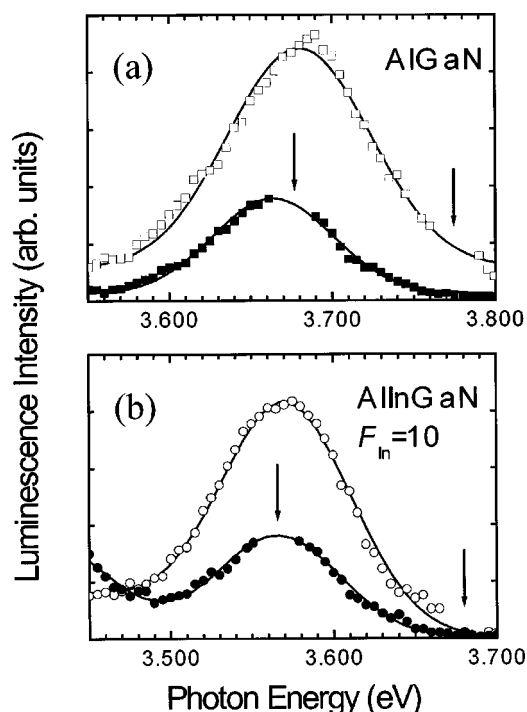


FIG. 1. Room-temperature luminescence spectra of AlGaIn (a) and AlInGaIn with $F_{\text{In}}=10 \mu\text{mol/min}$ (b) layers. Open points, off-resonant excitation; filled points, resonant excitation at the exciton energy (arrows indicate the incident photon energy). Solid lines, Gaussian approximation.

luminescence spectra for the samples grown with indium fluxes $F_{\text{In}}=0$ and $F_{\text{In}}=10 \mu\text{mol/min}$ are shown in Fig. 1. The data is presented for two incident pump energies. The solid dots in Fig. 1 are measured for the incident photon energies that coincide with the exciton energies extracted from the reflectivity spectra. The open dots correspond to the measurements for the incident photon energies that are approximately 100 meV above the exciton resonance. As seen from Fig. 1(a), the peak position of the resonantly excited luminescence band in AlGaIn is about 13 meV below the exciton energy. As discussed below, this peak blueshifts toward the exciton position with an increase in the excitation photon energy. In contrast, the peak position of the luminescence band in AlInGaIn samples (indium flows $F_{\text{In}}=5$ and $F_{\text{In}}=10 \mu\text{mol/min}$) is close to the exciton energy independently of the excitation photon energy.

Figure 2 shows the dependence of the luminescence band peak position on the incident photon energy (SSEPL data). In all investigated samples, a crossover from the anti-Stokes to Stokes luminescence is observed close to the exciton energy (indicated by arrows). The Stokes luminescence band in AlGaIn layers (upper points) monotonously shifts towards the higher energies. Such behavior of the luminescence band is characteristic for the localized-state filling in disordered systems.^{10,11} In contrast, no considerable shifting is observed in the quaternary AlInGaIn samples. We attribute the observed changes in the SSEPL to the indium-induced reduction of the band-tail states in the AlGaIn sublattice.

Our assumption about the reduction of the disorder in AlInGaIn is also supported by the PLE data presented in Fig. 3. These PLE spectra show spectrally integrated intensity of the photoluminescence band in AlGaIn and AlInGaIn layers as a function of the incident photon energy. The integral PLE

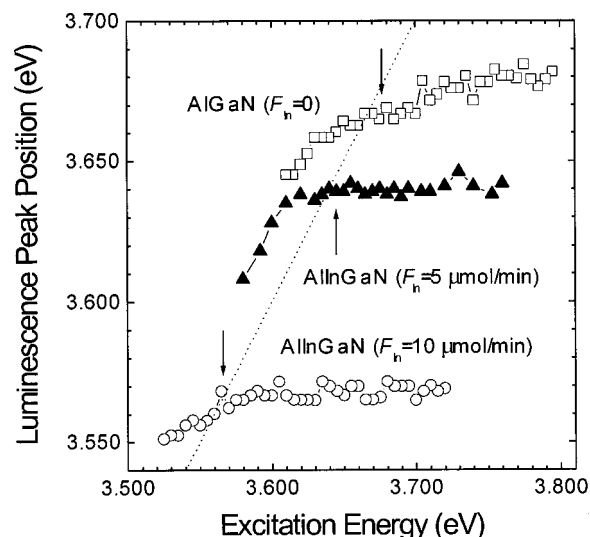


FIG. 2. Dependences of luminescence peak position on incident photon energy AlGaIn ($F_{\text{In}}=0$) and AlInGaIn ($F_{\text{In}}=5 \mu\text{mol/min}$ and $F_{\text{In}}=10 \mu\text{mol/min}$). Dotted line separates the Stokes region (left) from the anti-Stokes region (right). Arrows indicate exciton positions.

spectra of the buffer GaN layer are also shown in Fig. 3 for comparison. As seen from the figure, an Urbach tail is clearly observed below the exciton energy in AlGaIn layers. Above the exciton energy, the spectra exhibit a monotonous increase and saturation of the PL intensity. The energy region between the exciton energy and the saturation energy becomes smaller with incorporation of In. Note that in the buffer GaN layer, the saturation occurs immediately after passing the exciton energy (see Fig. 3).

We explain the difference between the PLE spectra of AlGaIn and AlInGaIn by the improved materials quality of the quaternary layers. The higher quality of AlInGaIn results not only in the reduction of the band-tail states but also leads to improved carrier transport characteristics. When the absorption length of the incident light is larger than the non-equilibrium carrier diffusion length, an increase in the excitation energy results in a higher light absorption, and, thus, in a higher density of carriers and excited tail states. This, in turn, yields a higher photoluminescence intensity. At the excitation energies corresponding to the onset of the PL saturation, the absorption length becomes comparable to or less

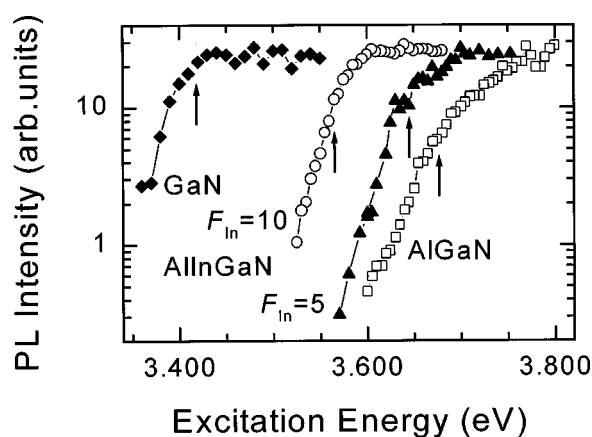


FIG. 3. Dependence of spectrally integrated luminescence intensity on incident photon energy in AlGaIn, AlInGaIn with $F_{\text{In}}=5 \mu\text{mol/min}$ and $F_{\text{In}}=10 \mu\text{mol/min}$, and GaN buffer layer. Arrows indicate exciton energies.

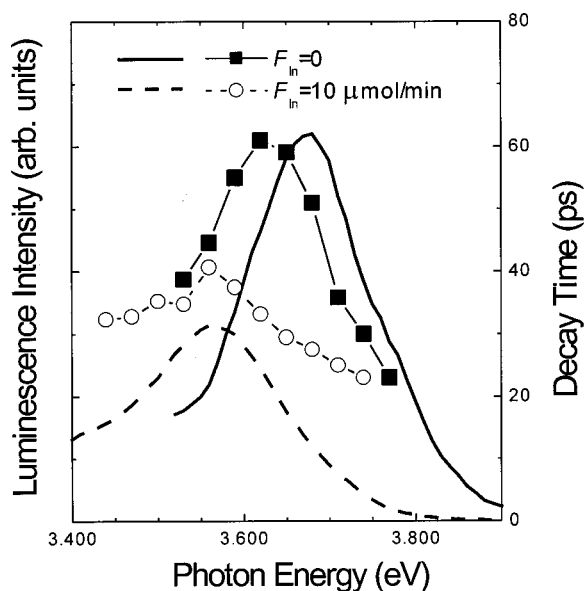


FIG. 4. Spectral distribution of luminescence decay time (points) and luminescence spectra (lines) in AlGaIn and AlInGaIn ($F_{\text{In}}=10 \mu\text{mol/min}$) layers.

than the diffusion length. In this regime, the nonequilibrium carrier density reaches its maximum value and stops growing. We should stress that the described behavior of PLE applies to the excitation with the constant number of incident photons.

In a partially disordered AlGaIn, the reduced carrier diffusivity and, probably, damped exciton resonance prevent the PLE spectra from saturation. With the incorporation of indium (quaternary AlInGaIn) the saturation is achieved earlier because of increased carrier diffusivity and reduced exciton damping. The diffusion length in a high-quality GaN buffer layer becomes larger than the absorption length at exciton energy. Therefore, we attribute the dynamics of the PLE spectra with increasing In molar fraction to (i) an increase in the carrier diffusivity associated with smoothing of the energy band potential profile, and (ii) the intensification of the band gap resonance.

The improvement in the crystal quality of the quaternary AlInGaIn with increase of In content was also supported by the TRL results. For TRL measurements, we used a frequency-quadrupled and mode-locked $\text{Nd}^{3+}:\text{YAG}$ laser (photon energy 4.66 eV, pulse duration 20 ps). The temporal resolution of the measurements close to 20 ps was achieved using a toluene optical Kerr shutter. Figure 4 shows the spectral dependence of the luminescence decay time in AlGaIn and quaternary AlInGaIn layers. The decay time, which was extracted from the exponential kinetics of the luminescence intensity in the late stage of the relaxation, is collated with the corresponding luminescence spectra. As seen from the figure, a shift of the decay-time spectra towards lower energies by more than 50 meV is observed in AlGaIn. We attribute this shift to the carrier localization effect in the band-tail states of a partially disordered crystal.^{10,12} With incorporation of In in quaternary AlInGaIn layers, the spectral distribution of the decay time flattens, the peak decay time decreases, and the shift disappears. These TRL features

point to a transition from a localized- to delocalized-carrier regime.

In conclusion, we have demonstrated that incorporation of a few percents of indium into AlGaIn significantly changes the band-edge optical properties of the layers. AlGaIn layers under study are partially disordered because (i) the layers were grown at reduced temperature and (ii) they are partially relaxed (since estimated critical thickness of the fully strained AlGaIn with 10% of Al is less than 200 nm). The chaotic potential distribution in AlGaIn causes the blue-shift of the luminescence band with increased incident photon energy (filling of the band-tail states), the occurrence of an unsaturated region in the PLE spectra (reduced carrier diffusivity due to the potential “roughness”), and the red-shift of the luminescence decay-time spectral distribution with respect to the luminescence band (carrier localization). The SSEPL, PLE, and TRL data indicate that the initial partial disorder, which is characteristic of the AlGaIn sublattice disappears with the incorporation of In. The improved structure of the alloy might be related to isoelectronic doping similar to that observed in GaN.^{5,6} An abrupt band gap is formed in AlInGaIn with approximately 2% of In, which corresponds to a nearly lattice-matched growth of $\text{Al}_{0.09}\text{In}_y\text{Ga}_{0.91-y}\text{N}$ on GaN. These results demonstrate a potential of energy gap and lattice engineering using the quaternary material system for the development of electronic and high-efficiency light-emitting devices.

The work at USC was supported by the Ballistic Missile Defense Organization under Army SSCD Contract No. DASG60-97-C 0066, monitored by Dr. Brian Strickland and Dr. Kepi Wu. One author (A.Ž.) acknowledges support from the NRC Twinning Program.

- ¹M. Asif Khan, J. W. Yang, G. Simin, R. Gaska, M. S. Shur, H. Zur Loye, G. Tamulaitis, A. Zukauskas, D. J. Smith, D. Chandrasekhar, and R. Bicknell-Tassius, *Appl. Phys. Lett.* **76**, 1161 (2000).
- ²M. Asif Khan, J. W. Yang, G. Simin, R. Gaska, M. S. Shur, and A. D. Bykhovski, *Appl. Phys. Lett.* **75**, 2806 (1999).
- ³V. Adivarahan, M. Shatalov, A. Lunev, J. W. Yang, G. Simin, and M. Asif Khan, Abstracts of the 6th Wide Bandgap III-Nitride Workshop, Richmond, VA, 12–15 March 2000.
- ⁴M. E. Aumer, S. F. LeBoeuf, F. G. McIntosh, and S. M. Bedair, *Appl. Phys. Lett.* **75**, 3315 (1999).
- ⁵S. Yamaguchi, M. Kariya, S. Nitta, H. Amano, and I. Akasaki, *Appl. Phys. Lett.* **75**, 4106 (1999).
- ⁶H. M. Chung, W. C. Chuang, Y. C. Pan, C. C. Tsai, M. C. Lee, W. H. Chen, W. K. Chen, C. I. Chiang, C. H. Lin, and H. Chang, *Appl. Phys. Lett.* **76**, 897 (2000).
- ⁷C. Kiselevski, J. Kruger, S. Ruvimov, T. Suski, J. W. Ager III, E. Jones, Z. Liliental-Weber, M. Rubin, E. R. Weber, M. D. Bremser, and R. F. Davis, *Phys. Rev. B* **54**, 17 745 (2000).
- ⁸L. Görgens, O. Ambacher, M. Stutzmann, C. Miskys, F. Scholz, and J. Off, *Appl. Phys. Lett.* **76**, 577 (2000).
- ⁹K. P. Korona, A. Wyszomolek, K. Pakula, R. Stepniewski, J. M. Baranowski, I. Grzegory, B. Lucznik, M. Wroblewski, and S. Porowski, *Appl. Phys. Lett.* **69**, 788 (1996).
- ¹⁰A. Satake, Y. Masumoto, T. Miyajima, T. Asatsuma, F. Nakamura, and M. Ikeda, *Phys. Rev. B* **57**, R2041 (1998).
- ¹¹A. Klochikhin, A. Reznitsky, S. Permogorov, T. Breitkopf, M. Grün, M. Hetterich, C. Klingshirn, V. Lyssenko, W. Langbein, and J. M. Hvam, *Phys. Rev. B* **59**, 12 947 (1999).
- ¹²H. S. Kim, R. A. Mair, J. Li, J. Y. Lin, and H. X. Jiang, *Appl. Phys. Lett.* **76**, 1252 (2000).